

Nonlinear Vibrations Analysis of Overhead Power Lines: A Beam With Mass–Spring–Damper–Mass Systems

Mohammad A. Bukhari

College of Science and Engineering,
Central Michigan University,
Mt. Pleasant, MI 48859
e-mail: bukha2m@cmich.edu

Oumar R. Barry

College of Science and Engineering,
Central Michigan University,
Mt. Pleasant, MI 48859
e-mail: barry1o@cmich.edu

This paper examines the nonlinear vibration of a single conductor with Stockbridge dampers. The conductor is modeled as a simply supported beam and the Stockbridge damper is reduced to a mass–spring–damper–mass system. The nonlinearity of the system stems from the midplane stretching of the conductor and the cubic equivalent stiffness of the Stockbridge damper. The derived nonlinear equations of motion are solved by the method of multiple scales. Explicit expressions are presented for the nonlinear frequency, solvability conditions, and detuning parameter. The present results are validated via comparisons with those in the literature. Parametric studies are conducted to investigate the effect of variable control parameters on the nonlinear frequency and the frequency response curves. The findings are promising and open a horizon for future opportunities to optimize the design of nonlinear absorbers. [DOI: 10.1115/1.4038807]

Keywords: overhead transmission lines, stockbridge damper, midplane stretching, perturbation methods, aeolian vibration

1 Introduction

Aeolian vibrations of overhead transmission lines have been a subject of study for many years. This type of vibration is caused by wind speed ranging between 1–7 m/s and is characterized to be a low-amplitude and high-frequency vibration. The frequency of vibration, depending on the conductor diameter and the wind speed, ranges from 3 to 150 Hz [1–3]. This vibration must be suppressed in order to avoid fatigue failure of the conductor. The vibration suppression can be achieved by installing stockbridge dampers on the conductor or reducing the cable tension [4].

Aeolian vibration of transmission lines have been investigated using the energy balance method in [4–7] and the method of impedance in Refs. [8–10]. More recent works on this topic are examined in Refs. [11] and [12]. In Ref. [11], both conductor and stockbridge damper are modeled as Euler–Bernoulli beams. In Ref. [12], however, the damper is replaced by an equivalent mass–spring–damper–mass system. It should be noted that the nonlinearity is neglected in both Refs. [11] and [12].

When the end conditions of the conductor (beam) are immovable, the vibration nonlinearity arises from midplane stretching. Therefore, linear equations are not sufficient to describe the vibration adequately. This type of nonlinearity which leads to weakly nonlinear differential equations has been reviewed by Nayfeh and Mook [13]. Nayfeh also reviewed perturbation techniques, which are used to solve weakly nonlinear problems [14].

The earlier consideration of a nonlinear beam with a mass–spring system is introduced by Dowell [15]. Pakdemirli and Nayfeh extended this work by including the effect of nonlinear stretching [16]. Furthermore, Barry et al. extended this work by considering axial tension and multi attached systems [17].

More recent works on nonlinear vibration of a beam with attached masses can be found in Refs. [18–22]. The study on linear vibration of a beam with suspended spring–mass systems is examined in Refs. [23–32]. The nonlinear vibration of beam with suspended spring–mass systems has been examined in Ref. [33]. However, the nonlinearity in this problem is only due to the spring stiffness (i.e., no midplane stretching).

Contributed by the Technical Committee on Vibration and Sound of ASME for publication in the JOURNAL OF VIBRATION AND ACOUSTICS. Manuscript received April 19, 2017; final manuscript received November 14, 2017; published online January 24, 2018. Assoc. Editor: Alper Erturk.

In the present study, a single conductor with stockbridge dampers is modeled as an Euler–Bernoulli beam coupled with a mass–spring–damper–mass systems. The conductor is subjected to a pretension and wind force. The nonlinearity is due to midplane stretching, damping, and spring stiffness. Considering the case of external primary resonance, the method of multiple scales is used to obtain an approximate analytical solution for the weakly nonlinear differential equations. Parametric studies are conducted to examine the effect of variable control parameters on the nonlinear frequency and frequency response curves.

2 Mathematical Model

Figure 1 depicts a schematic diagram for a single conductor with a stockbridge damper. Usually, two dampers are attached to the conductor near each end. The stockbridge damper can be reduced to an equivalent in-span mass–spring–damper–mass system as shown in Fig. 2. The conductor has a length L , a mass per unit length m , an axial rigidity EA , and a flexural rigidity EI . The equivalent damper has a clamped mass M_{ci} , an equivalent suspended mass M_{di} , a linear stiffness K_i , a cubic nonlinear stiffness q_i , and a dashpot damping coefficient C_{di} . For the left damper, the subscript i is equal to 1 and the damper is located at X_{s1} . The subscript $i = 2$ is for the right damper located at X_{s2} from the reference frame. The conductor is subjected to a pretension, T .

When neglecting the nonconservative forces, the Lagrangian for the combined system can be expressed, as

$$\begin{aligned} \mathcal{L} = & \sum_{i=0}^n \int_{x_{si}}^{x_{s(i+1)}} m \dot{W}_{i+1}^2 dx + \frac{1}{2} \sum_{i=1}^n M_{ci} \dot{W}_i(x_{si}, t) + \frac{1}{2} \sum_{i=1}^n M_{di} \dot{V}_i \\ & - \frac{1}{2} \sum_{i=0}^n \int_{x_{si}}^{x_{s(i+1)}} EI (W_{i+1}'')^2 dx \\ & - \frac{1}{2} \sum_{i=0}^n \int_{x_{si}}^{x_{s(i+1)}} (EA - T) \left(u'_{i+1} + \frac{1}{2} W_{i+1}^2 \right)^2 \\ & - \frac{1}{2} \sum_{i=1}^n K_i (W_i(x_i, t) - V_i)^2 - \frac{1}{4} \sum_{i=1}^n q_i (W_i(x_i, t) - V_i)^4 \\ & - \frac{1}{2} T \sum_{i=0}^n \int_{x_{si}}^{x_{s(i+1)}} W_{i+1}^2 dx \end{aligned} \quad (1)$$

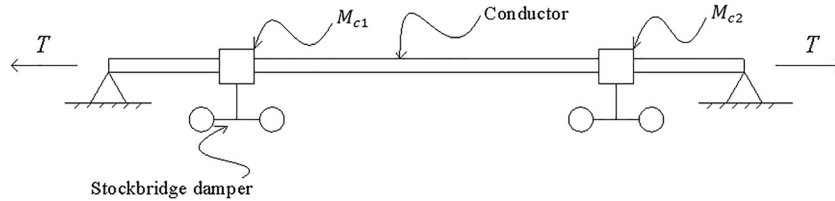


Fig. 1 Schematic of a single conductor with a stockbridge dampers

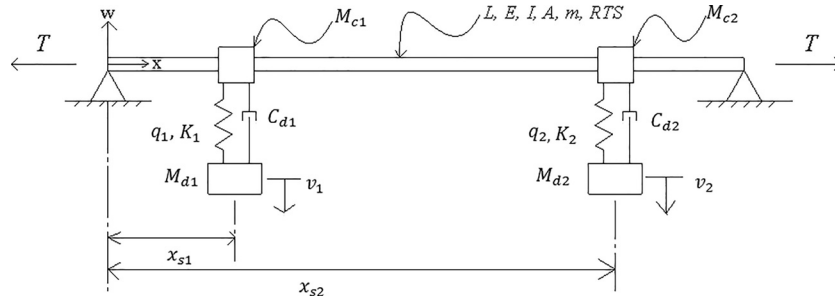


Fig. 2 Schematic of a simply supported beam with an in-span mass-spring-damper-mass systems

where W_i is the beam transverse displacement, u_i is the beam axial displacement, V_i is the absolute displacement of M_{di} , x is the axial coordinate, and n is the number of attached dampers. The dots and primes represent the temporal and spatial derivatives, respectively.

Introducing the Lagrangian into Hamilton's principle and adding the damping terms for the dampers yield the following nonlinear equations of motion and boundary conditions:

$$m\ddot{W}_{i+1} + EIW_{i+1}^{iv} - TW_{i+1}'' = \frac{EA - T}{2L} \left[\sum_{r=0}^n \int_{x_r}^{x_{r+1}} W_r'^2 dx \right] W_{i+1}'' \quad (2)$$

$$W_1(0, t) = W_1''(0, t) = 0 \quad (3)$$

$$W_{(n+1)}(0, t) = W_{(n+1)}''(0, t) = 0 \quad (4)$$

$$W_p(x_p, t) = W_{p+1}(x_p, t) \quad (5)$$

$$W_p'(x_p, t) = W_{p+1}'(x_p, t) \quad (6)$$

$$W_p''(x_p, t) = W_{p+1}''(x_p, t) \quad (7)$$

$$\begin{aligned} EI[W_p'''(x_p, t) - W_{p+1}'''(x_p, t)] \\ = M_{cp}\ddot{W}_p(x_p, t) + K_p(W_p(x_p, t) - V_p) \\ + q_p(W_p(x_p, t) - V_p)^3 + C_{dp}(\dot{W}_p(x_p, t) - \dot{V}_p) \end{aligned} \quad (8)$$

$$\begin{aligned} M_{dp}\ddot{V}_p = K_p(W_p(x_p, t) - V_p) \\ + q_p(W_p(x_p, t) - V_p)^3 + C_{dp}(\dot{W}_p(x_p, t) - \dot{V}_p) \end{aligned} \quad (9)$$

where $i = 0, 1, \dots, n$ and $p = 1, 2, \dots, n$. It is more convenient to introduce the following dimensionless variables:

$$\begin{aligned} \xi = \frac{x}{L}; \quad \xi_{i+1} = \frac{x_{s(i+1)}}{L}; \quad w_{i+1} = \frac{W_{i+1}}{r}; \quad \tau = \frac{t}{L^2} \sqrt{\frac{EI}{m}}; \\ \alpha_{1p} = \frac{M_{cp}}{mL}; \quad \alpha_{2p} = \frac{M_{dp}}{mL}; \quad k_p = \frac{K_p L^3}{EI}; \quad \gamma_p = \frac{q_p L^3 r^2}{EI}; \\ s = \sqrt{\frac{TL^3}{2EI}}; \quad \lambda = 1 - 2s^2 \frac{r^2}{l^2}; \quad \nu_p = \frac{V}{r}; \\ \alpha = \sqrt{-s^2 + \sqrt{s^4 + w^4}}; \quad \beta = \sqrt{s^2 + \sqrt{s^4 + w^4}}; \\ c_{dp} = \frac{C_{dp} l^2}{M_{dp}} \sqrt{\frac{m}{EI}} \end{aligned} \quad (10)$$

where r is the radius of gyration of the beam. Applying the dimensionless parameters into Eqs. (2)–(9) yields

$$\ddot{w}_{i+1} + w_{i+1}^{iv} - 2s^2 w_{i+1}'' = \frac{\lambda}{2} \left[\sum_{r=0}^n \int_{\xi_r}^{\xi_{r+1}} w_r'^2 d\xi \right] w_{i+1}'' \quad (11)$$

$$w_1(0, \tau) = w_1''(0, \tau) = 0 \quad (12)$$

$$w_{(n+1)}(0, \tau) = w_{(n+1)}''(0, \tau) = 0 \quad (13)$$

$$w_p(\xi_p, \tau) = w_{p+1}(\xi_p, \tau) \quad (14)$$

$$w_p'(\xi_p, \tau) = w_{p+1}'(\xi_p, \tau) \quad (15)$$

$$w_p''(\xi_p, \tau) = w_{p+1}''(\xi_p, \tau) \quad (16)$$

$$\begin{aligned} w_p'''(\xi_p, \tau) - w_{p+1}'''(\xi_p, \tau) \\ = \alpha_{1p}\ddot{w}_p(\xi_p, \tau) + k_p(w_p(\xi_p, \tau) - \nu_p) + \gamma_p(w_p(\xi_p, \tau) - \nu_p)^3 \\ + c_{dp}(\dot{w}_p(\xi_p, \tau) - \dot{\nu}_p) \end{aligned} \quad (17)$$

$$\begin{aligned} \alpha_{2p}\ddot{\nu}_p = k_p(w_p(\xi_p, \tau) - \nu_p) + \gamma_p(w_p(\xi_p, \tau) - \nu_p)^3 \\ + c_{dp}(\dot{w}_p(\xi_p, \tau) - \dot{\nu}_p) \end{aligned} \quad (18)$$

Adding the internal damping and the external forcing terms to Eq. (10) yields

$$\ddot{w}_{i+1} + w_{i+1}^{iv} - 2s^2 w_{i+1}'' = \frac{\lambda}{2} \left[\sum_{r=0}^n \int_{\xi_r}^{\xi_{r+1}} w_r^2 d\xi \right] w_{i+1}'' - 2\bar{\mu}\dot{w}_i + \bar{F}_i \cos \Omega t \quad (19)$$

where $\bar{\mu}$, \bar{F}_i , and Ω are, the dimensionless damping coefficient, the dimensionless drag force amplitude, and the dimensionless excitation frequency, respectively. Solution of Eqs. (12)–(19) is obtained using perturbation techniques. The method of multiple scale is applied directly to the partial differential equations and boundary conditions. Since the type of nonlinearity is cubic, one can assume the expansions of the displacements as

$$w_{i+1}(\xi, \tau, \epsilon) = \epsilon w_{(i+1)1}(\xi, T_0, T_2) + \epsilon^3 w_{(i+1)3}(\xi, T_0, T_2) + \dots \quad (20)$$

$$v_p(\tau, \epsilon) = \epsilon v_{p1}(T_0, T_2) + \epsilon^3 v_{p2}(T_0, T_2) + \dots \quad (21)$$

where ϵ is a small dimensionless book-keeping parameter. $T_0 = \tau$ and $T_2 = \epsilon^2 \tau$ are the fast and slow time scales, respectively. The term T_1 does not appear in the expansions, because the quadratic nonlinearity is missing in governing equations, so the effect of nonlinearity appears at $O(\epsilon^3)$. Since only the primary resonance case is considered in the current study, one can order the damping and excitation force as $\bar{\mu} = \epsilon^2 \mu$ and $\bar{F} = \epsilon^2 F_i$.

The dimensionless time derivatives in terms of partial derivatives with respect to each time scale T_n can be written as

$$(\cdot) = D_0 + \epsilon^2 D_2 \quad (22)$$

$$(\ddot{\cdot}) = D_0^2 + 2\epsilon^2 D_0 D_2 \quad (23)$$

where $D_n = (\partial/\partial T_n)$. Introducing the expansions of the displacements into Eqs. (12)–(19) and separating the coefficient of ϵ and ϵ^3 lead to

$$D_0^2 w_{(i+1)1} + w_{(i+1)1}^{iv} - 2s^2 w_{(i+1)1}'' = 0 \quad (24)$$

$$w_{11}(0, \tau) = w_{11}''(0, \tau) = 0 \quad (25)$$

$$w_{(n+1)1}(0, \tau) = w_{(n+1)1}''(0, \tau) = 0 \quad (26)$$

$$w_{p1}(\xi_p, \tau) = w_{(p+1)1}(\xi_p, \tau) \quad (27)$$

$$w_{p1}'(\xi_p, \tau) = w_{(p+1)1}'(\xi_p, \tau) \quad (28)$$

$$w_{p1}''(\xi_p, \tau) = w_{(p+1)1}''(\xi_p, \tau) \quad (29)$$

$$w_{p1}'''(\xi_p, \tau) - w_{(p+1)1}'''(\xi_p, \tau) = k_p(w_{p1}(\xi_p, \tau) - v_{p1}) + \alpha_{1p} D_0^2 w_{p1}(\xi_p, \tau) \quad (30)$$

$$\alpha_{2p} D_0^2 v_{p1} = k(w_{11}(\xi_p, \tau) - v_{p1}) \quad (31)$$

order ϵ^3

$$D_0^2 w_{(i+1)1} + w_{(i+1)1}^{iv} - 2s^2 w_{(i+1)1}'' = \frac{1}{2} \lambda \left[\sum_{r=0}^n \int_{\xi_r}^{\xi_{r+1}} w_{(r+1)1}^2 d\xi \right] w_{(i+1)1}'' - 2D_0 D_2 w_{(i+1)1} - 2\mu D_0 w_{(i+1)1} + F_{i+1} \cos \Omega T_0 \quad (32)$$

$$w_{13}(0, \tau) = w_{13}''(0, \tau) = 0 \quad (33)$$

$$w_{(n+1)3}(0, \tau) = w_{(n+1)3}''(0, \tau) = 0 \quad (34)$$

$$w_{p3}(\xi_p, \tau) = w_{(p+1)3}(\xi_p, \tau) \quad (35)$$

$$w_{p3}'(\xi_p, \tau) = w_{(p+1)3}'(\xi_p, \tau) \quad (36)$$

$$w_{p3}''(\xi_p, \tau) = w_{(p+1)3}''(\xi_p, \tau) \quad (37)$$

$$w_{p3}'''(\xi_p, \tau) - w_{(i+1)3}'''(\xi_p, \tau) = k_p(w_{p3}(\xi_p, \tau) - v_{p3}) + \gamma_p(w_{p1}(\xi_p, \tau) - v_{p1})^3 + c_{dp} D_0(w_{p1}(\xi_p, \tau) - v_{p1}) + \alpha_{1p} [D_0^2 w_{p3}(\xi_p, \tau) + 2D_0 D_2 w_{p1}(\xi_p, \tau)] \quad (38)$$

$$\alpha_{2p} [D_0^2 v_{p3} + 2D_0 D_2 v_{p1}] = k_p(w_{p3}(\xi_p, \tau) - v_{p3}) + \gamma_p(w_{p1}(\xi_p, \tau) - v_{p1})^3 + c_{dp} D_0(w_{p1}(\xi_p, \tau) - v_{p1}) \quad (39)$$

3 Linear Problem

The problem is linear at order ϵ Eqs. (24)–(31). The total linear system models are free harmonic vibrations, based on that, one can express the solution as [31]

$$w_{(i+1)1} = [A_1(T_2) e^{i\omega T_0} + cc] Y_{(i+1)}(\xi) \quad (40)$$

$$v_{p1} = A_{2p}(T_2) e^{i\omega T_0} + cc \quad (41)$$

where cc denotes to the complex conjugate of the preceding terms. Substituting Eqs. (40) and (41) into the linear model equations at order ϵ yields

$$Y_{i+1}^{iv} - \omega^2 Y_{i+1} = 0 \quad (42)$$

$$Y_1(0) = Y_1''(0) = 0 \quad (43)$$

$$Y_{n+1}(0) = Y_{n+1}''(0) = 0 \quad (44)$$

$$Y_p(\xi_p) = Y_{p+1}(\xi_p) \quad (45)$$

$$Y_p'(\xi_p) = Y_{p+1}'(\xi_p) \quad (46)$$

$$Y_p''(\xi_p) = Y_{p+1}''(\xi_p) \quad (47)$$

$$Y_p'''(\xi_p) - Y_{p+1}'''(\xi_p) = k_p \left(Y_p(\xi_p) - \frac{A_{2p}}{A_1} \right) - \omega^2 \alpha_{1p} Y_p(\xi_p) \quad (48)$$

$$-\alpha_{2p} \omega^2 A_{2p} = k_p (A_1 Y_p(\xi_p) - A_{2p}) \quad (49)$$

From Eq. (49), the function A_{2p} can be expressed in terms of A_1 as

$$A_{2p} = \Psi_p Y_p(\xi_p) A_1 \quad (50)$$

where Ψ_p is given by

$$\Psi_p = \frac{k_p}{k_p - \alpha_{2p} \omega^2} \quad (51)$$

The mode shapes of each portion from the beam can be represented as

$$Y_p = c_{1p} \sin \alpha \xi + c_{2p} \cos \alpha \xi + c_{3p} \sinh \beta \xi + c_{4p} \cosh \beta \xi \quad (52)$$

where $c_{1p}, c_{2p}, c_{3p}, c_{4p}$ are arbitrary constants, and α, β were defined in Eq. (10) as functions of the system's frequency. The values of the arbitrary constants and the natural frequencies of the system can be evaluated by applying the boundary conditions in Eqs. (43)–(49).

4 Nonlinear Problem

In contrary with the linear problem at order ϵ , the problem is nonlinear at order ϵ^3 . In order to obtain a solution for the nonhomogeneous Eqs. (32)–(39), the solvability condition must be satisfied [14]. To derive this condition, the solution should be assumed as

$$w_{(i+1)3} = \phi_{(i+1)}(\xi, T_2)e^{i\omega T_0} + cc + W_{i+1}^*(\xi, T_0, T_2) \quad (53)$$

$$v_{p3} = A_{3p}(T_2)e^{i\omega T_0} + cc + V_p^* \quad (54)$$

where $W_{i+1}^*(\xi, T_0, T_2)$ and V_p^* are unique, free of secular terms, and small divisor terms. Moreover, they can be determined by solving Eqs. (32)–(39) and deleting the terms accompanying $e^{\pm j\omega T_0}$.

Since we are attacking the primary resonance case, we consider that the excitation frequency is detuning from one of the natural frequencies by $\epsilon^2\sigma$ (σ is a detuning parameter), therefore, the excitation frequency can be represented by

$$\Omega = \omega + \epsilon^2\sigma \quad (55)$$

Introducing Eqs. (53) and (54) into Eqs. (32)–(39) and separating the terms that are coefficient of $e^{i\omega T_0}$ on both sides leads to

$$\begin{aligned} & \phi_{i+1}^{iv} - \omega^2\phi_{i+1} - 2s^2\phi_{i+1}'' \\ &= \frac{3}{2}\lambda\bar{A}_1A_1^2\left[\sum_{r=0}^n\int_{\xi_r}^{\xi_{r+1}}Y_{r+1}^2(\xi_r)d\xi\right]Y_{i+1}''(\xi) \\ & - 2j\omega(A_1' + \mu A_1)Y_{i+1}(\xi) + \frac{1}{2}F_{i+1}e^{i\sigma T_2} \end{aligned} \quad (56)$$

$$\phi_1(0, T_2) = \phi_1''(0, T_2) = 0 \quad (57)$$

$$\phi_{i+1}(0, T_2) = \phi_{i+1}''(0, T_2) = 0 \quad (58)$$

$$\phi_p(\xi_p, T_2) = \phi_{p+1}(\xi_p, T_2) \quad (59)$$

$$\phi_p'(\xi_p, T_2) = \phi_{p+1}'(\xi_p, T_2) \quad (60)$$

$$\phi_p''(\xi_p, T_2) = \phi_{p+1}''(\xi_p, T_2) \quad (61)$$

$$\begin{aligned} & \phi_p'''(\xi_p, T_2) - \phi_{p+1}'''(\xi_p, T_2) \\ &= k_p(\phi_p(\xi_p, T_2) - A_{p3}) + 3\gamma_p\Psi_{1p}A_1^2\bar{A}_1Y_p^3(\xi_p) \\ & + j\omega c_{dp}(A_1Y_p(\xi_p) - A_{p2}) + \alpha_{1p}[-\omega^2\phi_p(\xi_p, T_2) \\ & + 2j\omega A_1'Y_p(\xi_p)] \end{aligned} \quad (62)$$

$$\begin{aligned} & -\alpha_{2p}\omega^2A_{p3} + 2j\omega\alpha_{2p}A_{2p}' \\ &= k_p(\phi_p(\xi_p, T_2) - A_{p3}) + 3\gamma_p\Psi_{1p}A_1^2\bar{A}_1Y_p^3(\xi_p) \\ & + j\omega c_{dp}(A_1Y_p(\xi_p) - A_{p2}) \end{aligned} \quad (63)$$

where Ψ_{1p} is given by

$$\Psi_{1p} = -3\Psi_p^3 + 9\Psi_p^2 - 9\Psi_p + 1 \quad (64)$$

The term A_{p3} can be eliminated from Eq. (62) by rearranging Eq. (63), such that

$$\begin{aligned} A_{p3} &= \frac{K_p\phi_p(\xi_p, T_2) + 3A_1^2\bar{A}_1\Psi_{1p}\gamma_pY_p^3(\xi_p) - 2j\omega\alpha_{2p}\Psi_pY_p(\xi_p)A_1'}{K_p - \alpha_{2p}\omega^2} \\ & + \frac{j\omega c_{dp}A_1Y_p(\xi_p)(1 - \Psi_p)}{K_p - \alpha_{2p}\omega^2} \end{aligned} \quad (65)$$

Substituting Eqs. (50), (51), and (65) into Eq. (62) results in

$$\begin{aligned} & \phi_p'''(\xi_p, T_2) - \phi_{p+1}'''(\xi_p, T_2) \\ &= k_p(\phi_p(\xi_p, T_2)(1 - \Psi_p) + 3\gamma_p\Psi_{1p}A_1^2\bar{A}_1Y_p^3(\xi_p) \\ & - 3k_p\Psi_{2p}A_1^2\bar{A}_1 + j\omega k_p\Psi_{3p}A_1' + j\omega k_p\Psi_{4p}A_1(1 - \Psi_p) \\ & + j\omega c_{dp}Y_p(\xi_p)A_1(1 - \Psi_p) + \alpha_{1p}[-\omega^2\phi_p(\xi_p, \tau) + 2j\omega A_1'Y_p(\xi_p)]) \end{aligned} \quad (66)$$

where Ψ_{2p}, Ψ_{3p} , and Ψ_{4p} are defined as

$$\Psi_{2p} = \frac{\gamma_p\Psi_{1p}Y_p^3(\xi_p)}{k_p - \alpha_{2p}\omega^2} \quad (67)$$

$$\Psi_{3p} = \frac{2\alpha_{2p}\Psi_pY_p(\xi_p)}{k_p - \alpha_{2p}\omega^2} \quad (68)$$

$$\Psi_{4p} = \frac{c_{dp}Y_p(\xi_p)}{k_p - \alpha_{2p}\omega^2} \quad (69)$$

Manipulating Eqs. (56)–(61), and (66) algebraically leads to the following solvability condition:

$$\begin{aligned} & \frac{3}{2}\lambda\bar{A}_1A_1^2b_2b_3 - 2j\omega(A_1' + \mu A_1)b_1 + \frac{1}{2}e^{i\sigma T_2}f \\ &= \sum_{p=1}^2Y_p(\xi_p)\left[-3k_p\Psi_{2p}A_1^2\bar{A}_1 + j\omega k_p\Psi_{3p}A_1' \right. \\ & + j\omega k_p\Psi_{4p}A_1(1 - \Psi_p) + 3\gamma_p\Psi_{1p}A_1^2\bar{A}_1Y_p^3(\xi_p) \\ & \left. + j\omega c_{dp}Y_p(\xi_p)A_1(1 - \Psi_p) + 2j\omega\alpha_{1p}A_1'Y_p(\xi_p)\right] \end{aligned} \quad (70)$$

where the constants b_1, b_2, b_3 , and f are

$$b_1 = \sum_{r=0}^n\int_{\xi_r}^{\xi_{r+1}}Y_{r+1}^2d\xi \quad (71)$$

$$b_2 = \sum_{r=0}^n\int_{\xi_r}^{\xi_{r+1}}Y_{r+1}^{\prime 2}d\xi \quad (72)$$

$$b_3 = \sum_{r=0}^n\int_{\xi_r}^{\xi_{r+1}}Y_{r+1}''Y_{r+1}d\xi \quad (73)$$

$$f = \sum_{r=0}^n\int_{\xi_r}^{\xi_{r+1}}F_{r+1}Y_{r+1}d\xi \quad (74)$$

After integrating b_3 , it is found that $b_3 = -b_2$.

We express A_1 in the polar form

$$A_1(T_2) = \frac{1}{2}a(T_2)e^{i\theta(T_2)} \quad (75)$$

Moreover, in order to reach an autonomous system, we assume that

$$\gamma\gamma_1 = \sigma T_2 - \theta \quad (76)$$

Substituting Eqs. (75) and (76) into the solvability condition and separating the real and imaginary parts on both sides yields

$$\omega a' b_4 = \frac{1}{2} f \sin \gamma \gamma_1 - \omega b_5 a \quad (77)$$

$$\omega a (\sigma - \gamma \gamma_1') b_4 = -\frac{1}{2} f \cos \gamma \gamma_1 + a^3 b_5 \quad (78)$$

where b_4 , b_5 , and b_6 are defined as

$$b_4 = b_1 + \sum_{p=1}^n Y_p(\xi_p) \left[\frac{1}{2} k_p \Psi_{3p} + \alpha_{1p} Y_p(\xi_p) \right] \quad (79)$$

$$b_5 = \frac{3}{16} \lambda b_2^2 + \sum_{p=1}^n \left[-\frac{3}{8} k_p \Psi_{2p} Y_p(\xi_p) + \frac{3}{8} \gamma_p \Psi_{1p} Y_p^4(\xi_p) \right] \quad (80)$$

$$b_6 = \mu b_1 + \sum_{p=1}^n Y_p(\xi_p) \left[\frac{1}{2} k_p \Psi_{4p} (1 - \Psi_p) + \frac{1}{2} c_{dp} Y_p(\xi_p) (1 - \Psi_p) \right] \quad (81)$$

The nonlinear frequencies can be determined by assuming free undamped vibrations, such that $\sigma = f = \mu = c_{dp} = 0$, then Eqs. (77) and (78) become

$$a' = 0 \Rightarrow a = \text{constant} \quad (82)$$

$$\omega a b_4 \gamma \gamma_1' = -b_5 a^3 \quad (83)$$

Therefore, the nonlinear frequency can be expressed as

$$\omega_{nl} = \omega + \theta' \quad (84)$$

where θ' is the detuning from natural linear frequency and it can be defined as

$$\theta' = \frac{b_5 a^2}{\omega b_4} \quad (85)$$

It can be demonstrated that the motion type is periodic because a is a constant. This leads to $a' = \gamma \gamma_1' = 0$. The detuning parameter, therefore, can be written, after eliminating $\gamma \gamma_1$ from Eqs. (77) and (78), as

$$\sigma = \frac{a^2 b_5}{\omega b_4} \pm \sqrt{\frac{f^{*2}}{4a^2 \omega^2} - \frac{b_6^2}{b_4^2}} \quad (86)$$

where

$$f^* = \frac{f}{b_4} \quad (87)$$

The loci of the second saddle-node bifurcation point (i.e., where the tangent at this point from frequency response curve is vertical and the solution between this point and the first saddle-node bifurcation point is unstable) can be determined by solving the following equation:

$$\sigma^2 + 3 \frac{a^4 b_5^2}{\omega^2 b_4^2} - 4 \frac{\sigma a^2 b_5}{\omega b_4} + \frac{b_6^2}{b_4^2} = 0 \quad (88)$$

Following Ref. [34], the nonlinear component of the equivalent stiffness can be expressed as:

$$\gamma_p = k_p / 6 \quad (89)$$

5 Numerical Simulation

In order to check the current model, we compare the obtained natural frequencies for a conductor with one damper and for a beam with two masses with those obtained in the literature. The frequencies are tabulated in Tables 1 and 2 and show very good agreement. Moreover, the present results of nonlinear frequency response curve for a beam with one attached mass–spring system (i.e., no suspended mass) corroborate those in Ref. [17], as shown in Fig. 3.

Figures 4–9 depict the effect of various parameters on the nonlinear frequency with vibration amplitude a . The influence of changing the position of damper is shown in Fig. 4. It is demonstrated that the effect of nonlinearity increases as the number of dampers and ξ_p increase. It should be noted that stockbridge dampers are usually positioned near the end of the conductor because field investigations have shown that dampers placed further from the suspension clamps have increased tendency to suffer early fatigue failure due to galloping [35] and [36].

In Figs. 5 and 6, the nonlinear frequency–amplitude curves are plotted for different values of in-span mass and suspended mass, respectively. It is observed that the linear, nonlinear frequencies, and the nonlinearity of the curves decrease with increasing both masses. These results corroborate those obtained in Ref. [22]. For the case of the in-span mass shown in Fig. 5, it can be seen that the nonlinear frequency curve for $\alpha_{1p} = 0.01$ does not significantly

Table 1 Validating the natural frequencies (Hz) of a conductor with one damper for $\xi_1=0.05$, $\alpha_{11}=0.0045$, $\alpha_{21}=0.1088$, $k_1=17139.7$, and $s=80.33$

Data	First mode	Second mode	Third mode	Fourth mode	Fifth mode
Present	2.3634	2.6366	4.8244	7.2402	9.6696
FEM [12]	2.3845	2.6387	4.8164	7.2337	9.6663

Table 2 Validating the nondimensional natural frequencies (Hz) of a beam with two masses for $\xi_1=0.1$, $\xi_2=0.3$, $\alpha_{11}=1$, $\alpha_{12}=1$, and $s=k_1=k_2=0$

Data	First mode	Second mode	Third mode	Fourth mode	Fifth mode
Present	6.119	27.546	55.412	99.098	196.79
FEM [17]	6.1182	27.5061	55.4118	99.1006	196.8213

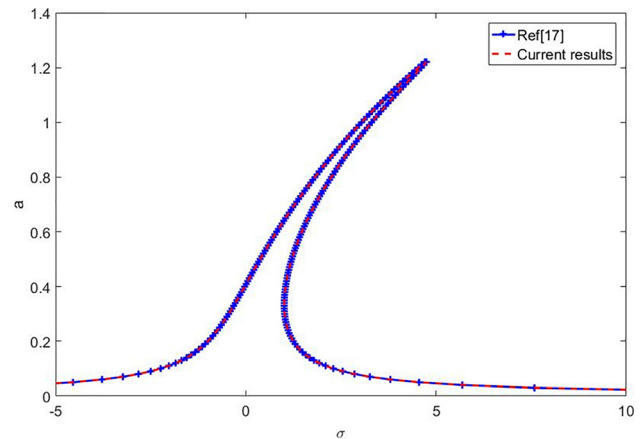


Fig. 3 Validating the current results: $s=0$, $\alpha_{11}=\alpha_{12}=0.5$, $\alpha_{21}=\alpha_{22}=0$, $k_p=\gamma_p=2\pi^4$, $\mu=0.2$, $v=0$

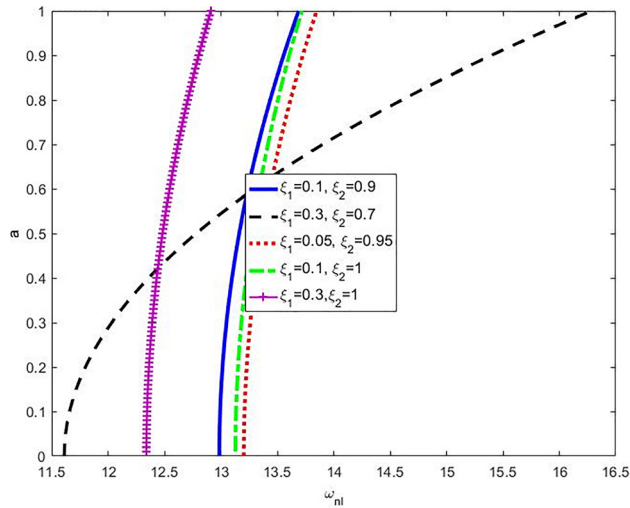


Fig. 4 Nonlinear frequency versus vibration amplitude for different dampers location: $s = 2$, $\alpha_{11} = \alpha_{12} = 0.01$, $\alpha_{21} = \alpha_{22} = 0.1$, $k_p = 2\pi^4$, $\gamma_p = k_p/6$

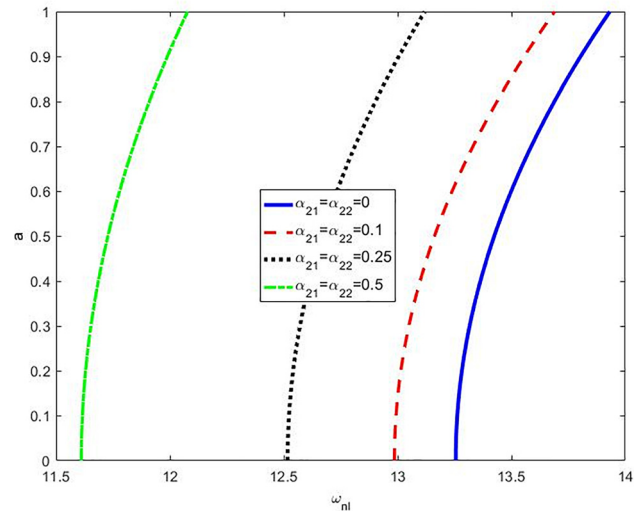


Fig. 6 Nonlinear frequency versus vibration amplitude for different suspended mass values: $s = 2$, $\xi_1 = 0.1$, $\xi_2 = 0.9$, $\alpha_{11} = \alpha_{12} = 0.01$, $k_p = 2\pi^4$, $\gamma_p = k_p/6$

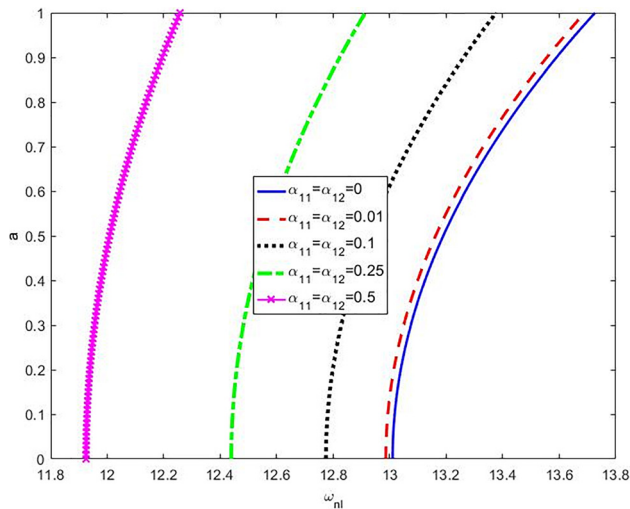


Fig. 5 Nonlinear frequency versus vibration amplitude for different in-span mass values: $s = 2$, $\xi_1 = 0.1$, $\xi_2 = 0.9$, $\alpha_{21} = \alpha_{22} = 0.1$, $k_p = 2\pi^4$, $\gamma_p = k_p/6$

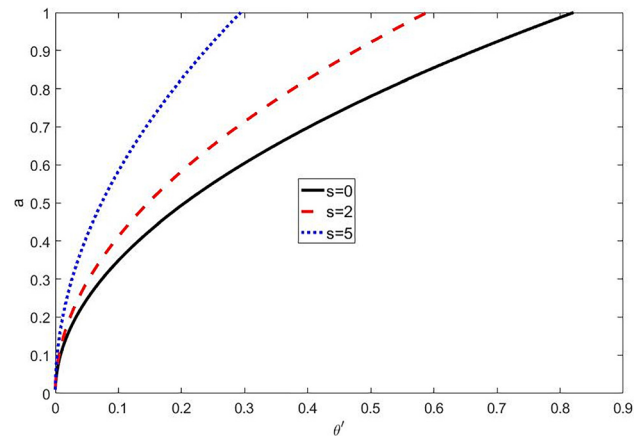


Fig. 7 Detuning from the linear natural frequency versus vibration amplitude for different values of tension: $\xi_1 = 0.1$, $\xi_2 = 0.9$, $\alpha_{11} = \alpha_{12} = 0.01$, $\alpha_{21} = \alpha_{22} = 0.1$, $k_p = 2\pi^4$, $\gamma_p = k_p/6$

differ from the bare beam curve (i.e., $\alpha_{1p} = 0$). However, for the suspended mass case depicted in Fig. 6, the difference is significant.

The effect of axial tension on the nonlinear frequency–amplitude curves is shown in Fig. 7. As expected, increasing the tension increases the linear and nonlinear frequencies. However, this increase in tension decreases the effect of nonlinearity in the curves which is reasonable since the term that includes nonlinear stretching in Eq. (2) becomes smaller.

Figures 8 and 9 illustrate the influence of varying the spring stiffness on the nonlinear frequency–amplitude curves. It is demonstrated that reducing the spring stiffness increases the frequencies and reduces the nonlinearity in the curves. Moreover, this effect becomes more pronounced as the suspended mass increases.

The frequency–response curves for variable parameters are plotted in Figs. 10–17, where the solid branches indicate stable solutions, while the dotted branch refers to unstable solutions. The effect of changing the axial tension is shown in Fig. 10. It is observed that increasing the tension reduces the hardening

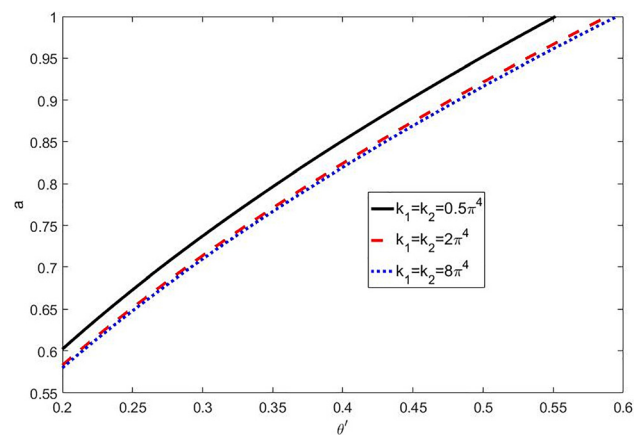


Fig. 8 Detuning from the linear natural frequency versus vibration amplitude for different values of spring stiffness: $s = 2$, $\xi_1 = 0.1$, $\xi_2 = 0.9$, $\alpha_{11} = \alpha_{12} = 0.01$, $\alpha_{21} = \alpha_{22} = 0.1$, $\gamma_p = k_p/6$

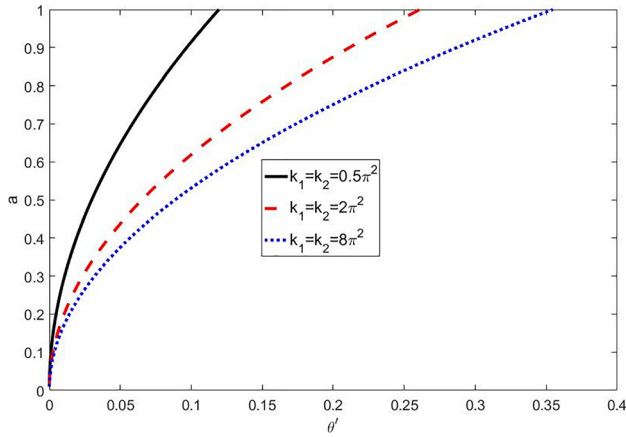


Fig. 9 Detuning from the linear natural frequency versus vibration amplitude for different values of spring stiffness: $s = 2$, $\xi_1 = 0.1$, $\xi_2 = 0.9$, $\alpha_{11} = \alpha_{12} = 0.01$, $\alpha_{21} = \alpha_{22} = 0.5$, $\gamma_p = k_p/6$

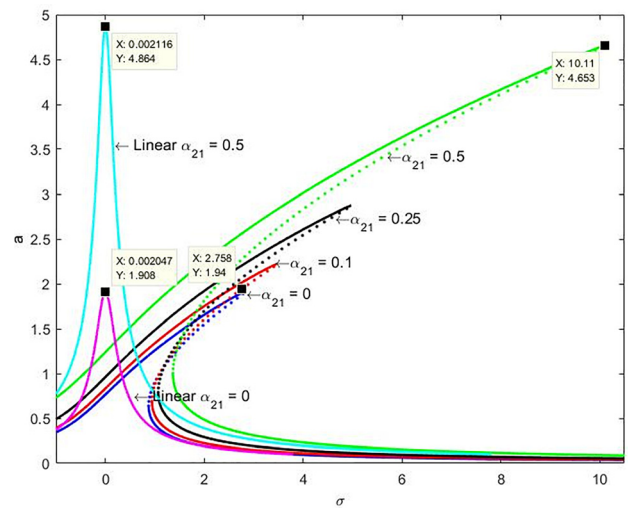


Fig. 12 Frequency-response curves for different values of suspended mass: $s = 2$, $\xi_1 = 0.1$, $\xi_2 = 0.9$, $\alpha_{11} = \alpha_{12} = 0.01$, $k_p = 2\pi^4$, $\gamma_p = k_p/6$, $f = 5$, $\mu = 0.2$

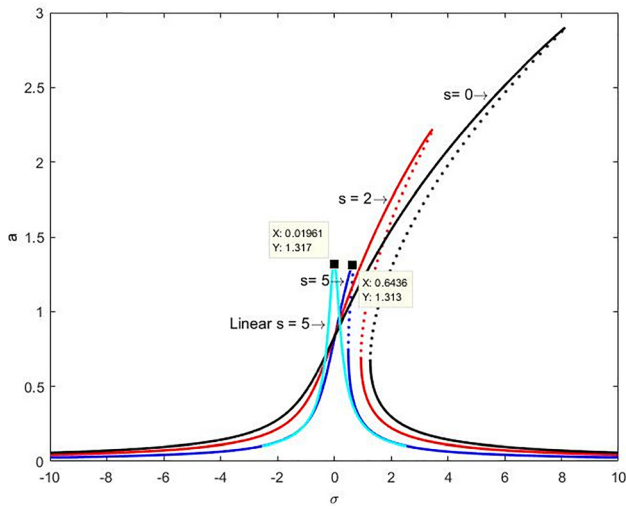


Fig. 10 Frequency-response curves for variables values of tension: $\xi_1 = 0.1$, $\xi_2 = 0.9$, $\alpha_{11} = \alpha_{12} = 0.01$, $\alpha_{21} = \alpha_{22} = 0.5$, $k_p = 2\pi^4$, $\gamma_p = k_p/6$, $f = 5$, $\mu = 0.2$

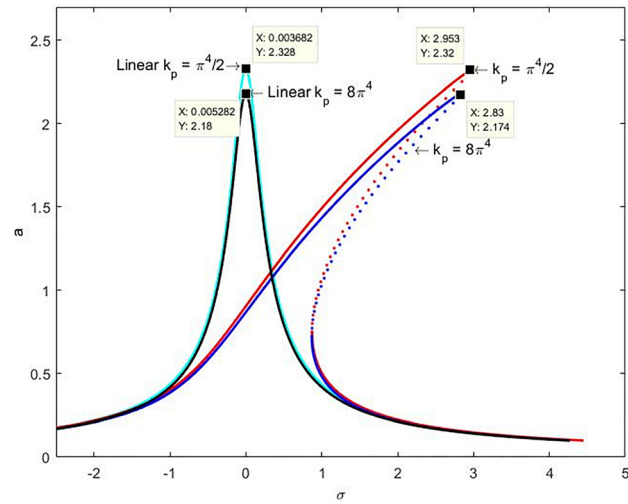


Fig. 13 Frequency-response curves for different values of spring stiffness: $s = 2$, $\xi_1 = 0.1$, $\xi_2 = 0.9$, $\alpha_{11} = \alpha_{12} = 0.01$, $\alpha_{21} = \alpha_{22} = 0.1$, $\gamma_p = k_p/6$, $f = 5$, $\mu = 0.2$

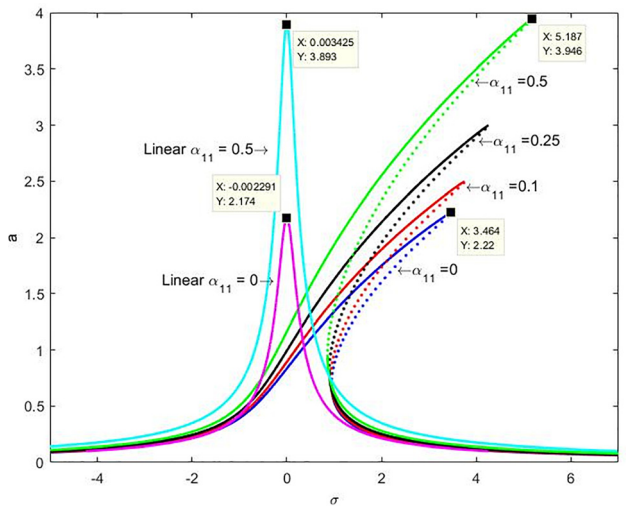


Fig. 11 Frequency-response curves for different values of in-span mass: $s = 2$, $\xi_1 = 0.1$, $\xi_2 = 0.9$, $\alpha_{21} = \alpha_{22} = 0.1$, $k_p = 2\pi^4$, $\gamma_p = k_p/6$, $f = 5$, $\mu = 0.2$

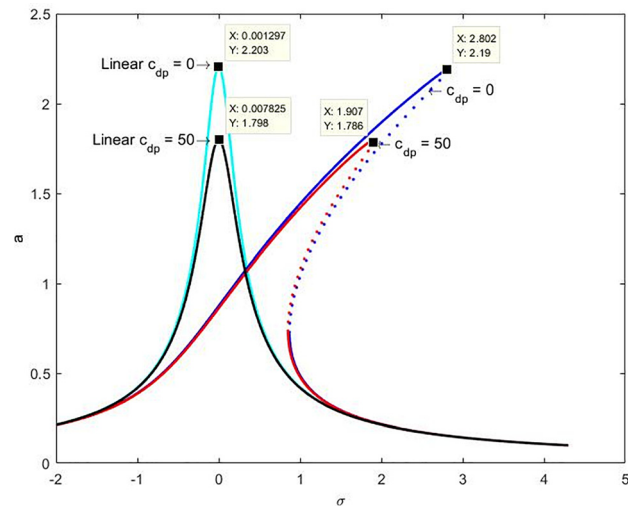


Fig. 14 Frequency-response curves for different values of damping: $s = 2$, $\xi_1 = 0.1$, $\xi_2 = 0.9$, $\alpha_{11} = \alpha_{12} = 0.01$, $\alpha_{21} = \alpha_{22} = 0.1$, $k_p = 2\pi^4$, $\gamma_p = k_p/6$, $f = 5$, $\mu = 0.2$

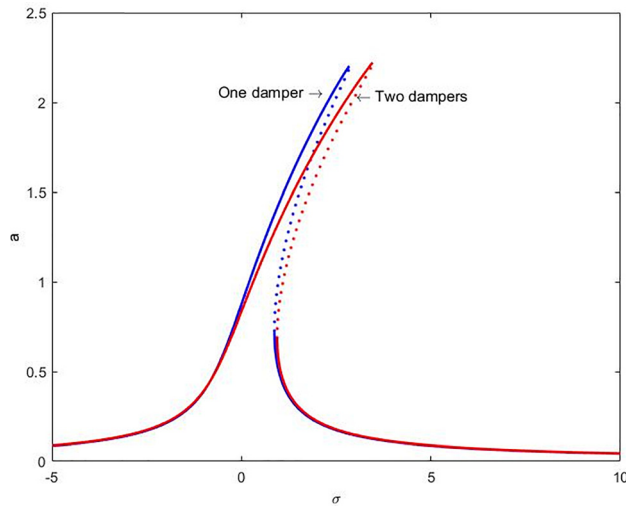


Fig. 15 Frequency–response curves for a conductor with one and two dampers (no damping): $s = 2$, $\xi_1 = 0.1$, $\xi_2 = 0.9$, $\alpha_{11} = \alpha_{12} = 0.01$, $\alpha_{21} = \alpha_{22} = 0.1$, $k_p = 2\pi^4$, $\gamma_p = k_p/6$, $\mu = 0.2$, $f = 5$

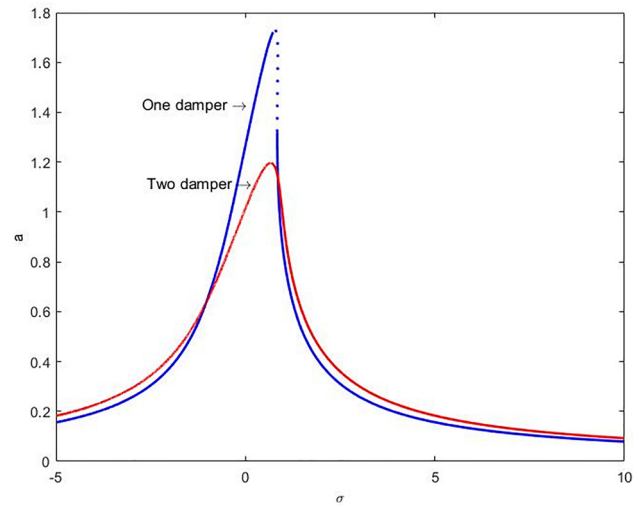


Fig. 17 Frequency–response curves for a conductor with one and two dampers (with damping $c_{dp} = 10$): $s = 2$, $\xi_1 = 0.1$, $\xi_2 = 0.9$, $\alpha_{11} = \alpha_{12} = 0.01$, $\alpha_{21} = \alpha_{22} = 0.5$, $k_p = 2\pi^4$, $\gamma_p = k_p/6$, $\mu = 0.2$, $f = 5$

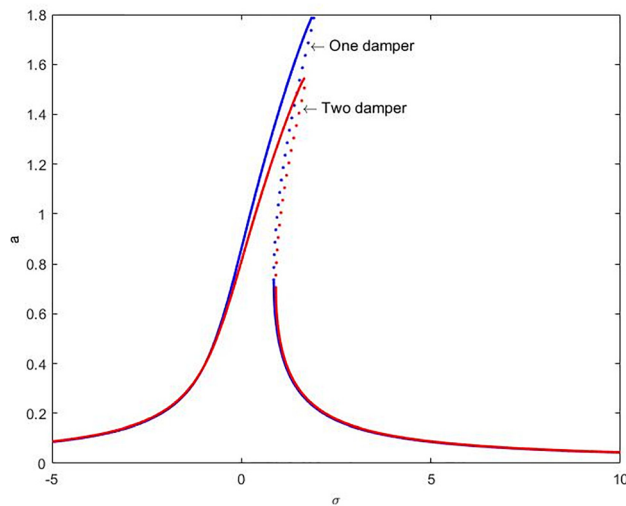


Fig. 16 Frequency–response curves for a conductor with one and two dampers (with damping $c_{dp} = 50$): $s = 2$, $\xi_1 = 0.1$, $\xi_2 = 0.9$, $\alpha_{11} = \alpha_{12} = 0.01$, $\alpha_{21} = \alpha_{22} = 0.1$, $k_p = 2\pi^4$, $\gamma_p = k_p/6$, $\mu = 0.2$, $f = 5$

nonlinearity. In comparison to the linear case, the midplane stretching shifts the resonance peak to the right; however, this shift to the right reduces with increasing tension.

Figures 11 and 12 depict the frequency response curves for variable values of in-span mass and suspended mass, respectively. The results reveal that raising any of these masses increases the maximum amplitude of the vibration for both linear and nonlinear absorbers. The results in Fig. 11 indicate a slightly higher vibration amplitude for the nonlinear absorber than the linear absorber, whereas the results in Fig. 12 show opposite trends. This is an indication that the nonlinear absorber performs better with increasing the suspended mass than increasing the in-span mass. Increasing the stiffness of the damper also increases the maximum amplitude as shown in Fig. 13. The effect of increasing damping on the maximum amplitude is plotted in Fig. 14. The results show that higher damping decreases the vibration amplitude. In terms of reducing vibration amplitudes, both Figs. 13 and 14 show that the nonlinear absorber performs better than the linear absorber.

A comparison between a conductor with one damper and two dampers along with different parameters are shown in

Figs. 15–17. For an absorber with zero damping coefficient, it is observed that the maximum amplitude of a conductor with one damper is slightly lower than that for a conductor with two dampers as depicted in Fig. 15. However, it is demonstrated from Fig. 16 that the maximum displacement becomes lower as the number of absorber increases for nonzero damping coefficient. These findings agree with those in Ref. [36] for linear absorbers. Moreover, it is revealed that increasing the suspended mass also lowers the maximum displacement for a conductor with more than one damper even for a lower value of damping as shown in Fig. 17.

6 Conclusion

In this paper, the nonlinear vibration of an overhead transmission line consisting of a single conductor with stockbridge dampers is investigated. The conductor is modeled as simply supported beam and the stockbridge damper is represented as a mass–spring–damper–mass system. The nonlinearity is due to midplane stretching of the beam and cubic nonlinearity of the spring stiffness. The nonlinear differential equations of motion, boundary, and continuity conditions are derived using Hamilton’s principle. The system of weakly nonlinear differential equations is solved using the method of multiple scales. Explicit expressions are presented for the nonlinear frequency, solvability conditions, and detuning parameter. The validation of the present results is demonstrated via comparison of the results in the literature. The numerical simulation demonstrates that the nonlinearity increases with increasing number of absorbers and moving them toward the midpoint of the beam. It is observed that both linear and nonlinear frequencies decrease with increasing inspan mass and suspended mass, and decreasing tension. The nonlinearity in the frequency curves becomes more noticeable with decreasing tension and spring stiffness.

As for the frequency–response curves, the results indicate that the effect of nonlinearity vanishes with increasing tension. Moreover, it is shown that increasing the masses increases the maximum vibration amplitude, while increasing the damping and the stiffness of the absorbers reduces the vibration amplitude. The numerical results also reveal that the maximum vibration amplitude decreases with increasing suspended mass, damping coefficient, and the number of absorbers. The results also demonstrate that nonlinear absorbers perform better than linear absorbers. The findings in this paper provide fundamental insights about nonlinear absorbers and pave the way for future research to optimize their performance. It is also anticipated that the findings will

be very appealing to power lines engineers and manufacturers of stockbridge dampers.

Nomenclature

α = dimensionless first Eigen value
 α_{1p} = dimensionless in span mass for the p th absorber
 α_{2p} = dimensionless suspended mass for the p th absorber
 β = dimensionless second Eigen value
 ϵ = book-keeping parameter
 θ = dimensionless vibration phase
 λ = dimensionless coefficient of nonlinear terms
 $\bar{\mu}$ = dimensionless internal damping coefficient of the beam
 μ = dimensionless ordered internal damping coefficient of the beam
 σ = detuning parameter
 ξ = dimensionless horizontal coordinate
 ξ_i = dimensionless position for the i th absorber
 Ω = dimensionless forcing frequency
 ω = dimensionless natural frequency of the system
 a = dimensionless vibration amplitude
 A_1 = unknown complex function at first-order
 A_{2p} = unknown complex function at first-order
 c_{dp} = dimensionless damping coefficient for the p th absorber
 cc = complex conjugate
 C_{dp} = damping coefficient for the i th absorber ((N s)/m)
 D_n = first derivative with respect to n th scale
 EA = axial rigidity (N)
 EI = flexural rigidity (N m²)
 F_i = dimensionless ordered force amplitude for the i th beam
 \bar{F}_i = dimensionless force amplitude for the i th beam
 k_p = dimensionless linear stiffness for the p th absorber
 K_i = linear stiffness for the i th absorber (N/m)
 \mathcal{L} = Lagrangian of the combined system
 L = length of the beam (m)
 m = mass per unit length of the beam (kg/m)
 M_{ci} = in span mass for the i th absorber (kg)
 M_{di} = suspended mass for the i th absorber (kg)
 n = number of attached systems
 q_i = nonlinear stiffness for the i th absorber (N/m³)
 τ = dimensionless time
 r = radius of gyration (m)
 s = dimensionless axial tension
 T = axial tension (N)
 T_0 = fast-time scale
 T_1 = slow-time scale
 u_i = axial displacement for the i th beam (m)
 v_p = dimensionless absolute displacement for the p th absorber
 v_{p1} = dimensionless first-order solution for the displacement of p th absorber
 v_{p3} = dimensionless third-order solution for the displacement of p th absorber
 V_i = absolute displacement for the i th absorber (m)
 V_p^* = unique terms at third-order
 w_{i1} = dimensionless first-order solution for the displacement of i th beam
 w_{i3} = dimensionless third-order solution for the displacement of i th beam
 W_i = transverse displacement of the i th beam (m)
 W_i^* = unique terms at third-order
 x_{si} = position of i th absorber on the beam (m)
 Y_i = linear mode shape for the i th beam
 γ_p = dimensionless nonlinear stiffness for the p th absorber
 $\gamma\gamma_1$ = autonomous transfer parameter

References

[1] Chan, J., Harvard, D., Rawlins, C., Diana, G., Cloutier, L., Lilien, J., Hardy, C., Wang, J., and Goel, A., 2009, *EPRI Transmission Line Reference Book: Wind-Induced Conductor Motion*, Electric Power Research Institute, Palo Alto, CA.

[2] Barry, O., Zu, J. W., and Oguamanam, D. C. D., 2015, "Analytical and Experimental Investigation of Overhead Transmission Line Vibration," *J. Vib. Control*, **21**(14), pp. 2825–2837.

[3] Barry, O., Oguamanam, D. C., and Lin, D. C., 2013, "Aeolian Vibration of a Single Conductor With a Stockbridge Damper," *Proc. Inst. Mech. Eng. Part C*, **227**(5), pp. 935–945.

[4] Oliveira, A. R., and Freire, D. G., 1994, "Dynamical Modelling and Analysis of Aeolian Vibrations of Single Conductors," *IEEE Trans. Power Delivery*, **9**(3), pp. 1685–1693.

[5] Verma, H., and Hagedorn, P., 2005, "Wind Induced Vibrations of Long Electrical Overhead Transmission Line Spans: A Modified Approach," *Wind Struct.*, **8**(2), pp. 89–106.

[6] Schfer, B., 1984, "Dynamical Modelling of Wind-Induced Vibrations of Overhead Lines," *Int. J. Non-Linear Mech.*, **19**(5), pp. 455–467.

[7] Kraus, M., and Hagedorn, P., 1991, "Aeolian Vibrations: Wind Energy Input Evaluated From Measurements on an Energized Transmission Line," *IEEE Trans. Power Delivery*, **6**(3), pp. 1264–1270.

[8] Tompkins, J. S., Merrill, L. L., and Jones, B. L., 1956, "Quantitative Relationships in Conductor Vibration Damping," *Trans. Am. Inst. Electr. Eng. Part III*, **75**(3), pp. 879–896.

[9] Nigol, O., Heics, R. C., and Houston, H. J., 1985, "Aeolian Vibration of Single Conductors and Its Control," *IEEE Trans. Power Apparatus Syst.*, **PAS-104**(11), pp. 3245–3254.

[10] Rawlins, C. B., 1958, "Recent Developments in Conductor Vibration Research," Alcoa Research Laboratories, Pittsburgh, PA, Technical Paper No. 13.

[11] Barry, O., Zu, J. W., and Oguamanam, D. C. D., 2014, "Forced Vibration of Overhead Transmission Line: Analytical and Experimental Investigation," *ASME J. Vib. Acoust.*, **136**(4), p. 041012.

[12] Barry, O., Long, R., and Oguamanam, D. C. D., 2016, "Simplified Vibration Model and Analysis of a Single-Conductor Transmission Line With Dampers," *Proc. Inst. Mech. Eng., Part C*, **231**(11), pp. 4150–4162.

[13] Nayfeh, A. H., and Mook, D. T., 1979, *Nonlinear Oscillations*, Wiley, New York.

[14] Nayfeh, A. H., 1981, *Introduction to Perturbation Techniques*, Wiley, New York.

[15] Dowell, E. H., 1980, "Component Mode Analysis of Nonlinear and Nonconservative Systems," *ASME J. Appl. Mech.*, **47**(1), pp. 172–176.

[16] Pakdemirli, M., and Nayfeh, A. H., 1994, "Nonlinear Vibrations of a Beam-Spring-Mass System," *ASME J. Vib. Acoust.*, **116**(4), pp. 433–439.

[17] Barry, O. R., Oguamanam, D. C. D., and Zu, J. W., 2014, "Nonlinear Vibration of an Axially Loaded Beam Carrying Multiple Massspringdamper Systems," *Nonlinear Dyn.*, **77**(4), pp. 1597–1608.

[18] Low, K. H., 1997, "Comments on 'Non-Linear Vibrations of a Beam-Mass System Under Different Boundary Conditions' (With Authors' Reply)," *J. Sound Vib.*, **207**(2), pp. 284–287.

[19] Mestrom, R. M. C., Fey, R. H. B., Phan, K. L., and Nijmeijer, H., 2010, "Simulations and Experiments of Hardening and Softening Resonances in a Clampedclamped Beam MEMS Resonator," *Sens. Actuators A: Phys.*, **162**(2), pp. 225–234.

[20] Ozkaya, E., and Pakdemirli, M., 1999, "Non-Linear Vibrations of a Beam-mass System With Both Ends Clamped," *J. Sound Vib.*, **221**(3), pp. 491–503.

[21] Ozkaya, E., Pakdemirli, M., and Öz, H. R., 1997, "Non-Linear Vibrations of a Beam-Mass System Under Different Boundary Conditions," *J. Sound Vib.*, **199**(4), pp. 679–696.

[22] Ozkaya, E., 2002, "Non-Linear Transverse Vibrations of a Simply Supported Beam Carrying Concentrated Masses," *J. Sound Vib.*, **257**(3), pp. 413–424.

[23] Lin, H. Y., and Tsai, Y. C., 2007, "Free Vibration Analysis of a Uniform Multi-Span Beam Carrying Multiple Springmass Systems," *J. Sound Vib.*, **302**(3), pp. 442–456.

[24] Hassanpour, P. A., Cleghorn, W. L., Mills, J. K., and Esmailzadeh, E., 2007, "Exact Solution of the Oscillatory Behavior Under Axial Force of a Beam With a Concentrated Mass Within Its Interval," *J. Vib. Control*, **13**(12), pp. 1723–1739.

[25] Naguleswaran, S., 2001, "Transverse Vibrations of an EulerBernoulli Uniform Beam Carrying Two Particles In-Span," *Int. J. Mech. Sci.*, **43**(12), pp. 2737–2752.

[26] Wu, J. S., and Lin, T. L., 1990, "Free Vibration Analysis of a Uniform Cantilever Beam With Point Masses by an Analytical-and-Numerical-Combined Method," *J. Sound Vib.*, **136**(2), pp. 201–213.

[27] Grgze, M., 1998, "On the Alternative Formulations of the Frequency Equation of a BernoulliEuler Beam to Which Several Spring-Mass Systems Are Attached in-Span," *J. Sound Vib.*, **217**(3), pp. 585–595.

[28] Barry, O. R., Zhu, Y., Zu, J. W., and Oguamanam, D. C. D., 2012, "Free Vibration Analysis of a Beam Under Axial Load Carrying a Mass-Spring-Mass," *ASME Paper No. DETC2012-70144*.

[29] Kirk, C. L., and Wiedemann, S. M., 2002, "Natural Frequencies and Mode Shapes of a Freefree Beam With Large End Masses," *J. Sound Vib.*, **254**(5), pp. 939–949.

[30] Wu, J. S., and Huang, C. G., 1995, "Free and Forced Vibrations of a Timoshenko Beam With Any Number of Translational and Rotational Springs and Lumped Masses," *Int. J. Numer. Methods Biomed. Eng.*, **11**(9), pp. 743–756.

[31] Wu, J.-S., and Chou, H.-M., 1998, "Free Vibration Analysis of a Cantilever Beam Carrying any Number of Elastically Mounted Point Masses With the Analytical-And-Numerical-Combined Method," *J. Sound Vib.*, **213**(2), pp. 317–332.

[32] Bokaian, A., 1990, "Natural Frequencies of Beams Under Tensile Axial Loads," *J. Sound Vib.*, **142**(3), pp. 481–498.

- [33] Samani, F. S., Pellicano, F., and Masoumi, A., 2013, "Performances of Dynamic Vibration Absorbers for Beams Subjected to Moving Loads," *Nonlinear Dyn.*, **73**(1–2), pp. 1065–1079.
- [34] Boisseau, S., Despesse, G., and Seddik, B. A., 2013, "Nonlinear H-Shaped Springs to Improve Efficiency of Vibration Energy Harvesters," *ASME J. Appl. Mech.*, **80**(6), p. 061013.
- [35] Bukhari, M. A., Barry, O., and Tanbour, E., 2017, "On the Vibration Analysis of Power Lines With Moving Dampers," *J. Vib. Control*, epub.
- [36] Barry, O., Long, R., and Oguamanam, D. C. D., 2017, "Rational Damping Arrangement Design for Transmission Lines Vibrations: Analytical and Experimental Analysis," *ASME J. Dyn. Syst. Meas. Control*, **139**(5), p. 051012.